Short-scale variations of shear-wave splitting across the Dead Sea basin: Evidence for the effects of sedimentary fill

Ayoub Kaviani,[1] Georg Rümpker,[1] Michael Weber,[2] and Günter Asch[2]

Received 14 December 2010; revised 21 January 2011; accepted 28 January 2011; published 26 February 2011.

[1] We examine shear-wave splitting of SKS waveforms collected by a temporary array of 68 stations in the region of the Dead Sea basin. The observed splitting parameters exhibit systematic variations along a dense, EW-trending 60 km profile across the basin. The delay times vary significantly between 1.0 and 2.8 seconds with smaller values in the very center of the profile. The fast polarizations are oriented more-or-less parallel to the strike of the Dead Sea transform fault and vary between −10 and 20 degrees with respect to North. Finite-frequency waveform modeling reveals that the source-region of the small-scale lateral variations is likely located within the crust. The modeling further shows that purely isotropic velocity variations affect shear-wave splitting: To a large degree, the observed variations of splitting parameters can be explained by the sedimentary fill of the basin and its low isotropic seismic velocities, whereas the mantle is uniformly anisotropic. Our study indicates that precaution must be taken when interpreting short-scale lateral variations of shear wave splitting in terms of anisotropic structures in the crust or upper mantle. **Citation:** Kaviani, A., G. Rümpker, M. Weber, and G. Asch (2011), Short-scale variations of shear-wave splitting across the Dead Sea basin: Evidence for the effects of sedimentary fill, *Geophys. Res. Lett.*, *38*, L04308, doi:10.1029/2010GL046464.

1. Introduction

[2] The Dead Sea Transform Fault (DST) is an approximately 1100 km long transform fault that connects the Red Sea spreading zone with the Zagros-Taurus continental collision zone to the north (Figure 1). It separates the Arabian and Sinai plates and has accommodated approximately 105 km of sinistral relative motion between the African and the Eurasian plate since the Early Miocene [e.g., *Garfunkel*, 1981]. The lateral left-step motion along the fault resulted in the formation of deep pull-apart basins. The Dead Sea Basin (DSB) is the most prominent among them and one of the largest on Earth. The DSB, about 150 km long and 10–17 km wide, is filled with Neogene to recent sediments with thicknesses varying from 6 km in the northern part to 12–15 km in the southern part; its boundaries are demarcated by sub-vertical faults. The velocity models obtained by seismic studies suggest the presence of anomalous low velocities beneath the DSB that, in the southern part of the basin, may extend to a depth of 18 km [*Ben-Avraham et al.*, 2008; *ten Brink et al.*, 2006; *Mechie et al.*, 2009].

[3] Previous seismological and magnetotelluric studies of the DST to the south of the basin [*Rümpker et al.*, 2003; *Weber et al.*, 2009] in conjunction with thermo-mechanical modeling [*Sobolev et al.*, 2005] provide evidence for a narrow vertical shear zone extending through the entire lithosphere as a result of the sinistral motion between the African and Arabian plate. A major goal of the deployment of seismological stations across the DSB is the study of mantle deformation processes associated with the development of the Dead Sea pull-apart basin. The analysis of shear-wave splitting based on teleseismic phases is a commonly used method to study upper mantle anisotropy related to the strain-induced lattice-preferred orientation of mantle minerals. In our study, the dense deployment, with distances of 2 km and less between neighboring stations, allows the application of finite-frequency waveform modeling to interpret the observations. In this approach, the two splitting parameters (the delay time, δt, between the two split shear waves and the polarization direction, ϕ, of the faster component) obtained at a single station are not directly interpreted but are used to quantify waveform effects and to deduce suitable models of crustal and upper-mantle anisotropy that agree with the observations.

2. Data and Analysis

[4] We exploited data from 72 teleseismic events collected by 29 broad-band and 39 short-period stations operated between October 2006 and March 2008 across the DSB within the framework of the multidisciplinary DESIRE project. After correcting for instrument responses, we utilize the analysis of shear-wave splitting of teleseismic core-refracted phases (SKS, SKKS and PKS) within a period range between 4 and 20 s to examine seismic anisotropy. We employ transverse-component minimization [*Silver and Chan*, 1991] to estimate the shear-wave splitting parameters and cross-checked the results by comparison with the cross-correlation method [*Bowman and Ando*, 1987]. We subsequently select those estimates for which the two methods yield consistent values at 95% confidence based on the χ^2 test. Our observations consist of 691 shear wave splitting estimates of reliable quality. In Figure 1, we show averaged splitting parameters at each station. The delay times vary between 1.0 and 2.8 seconds and are among the highest observed worldwide. The fast polarizations are oriented more-or-less parallel to the strike of the Dead Sea transform fault and range between −10° and 20° with respect to North. Individual observed splitting parameters at 52 stations from 4 events in backazimuth ranges 62° to 64° are provided as

[1]Geophysics Section, Institute of Geosciences, Goethe-University Frankfurt, Frankfurt, Germany.
[2]Deutsches GeoForschungsZentrum Potsdam, Potsdam, Germany.

0094-8276/11/2010GL046464

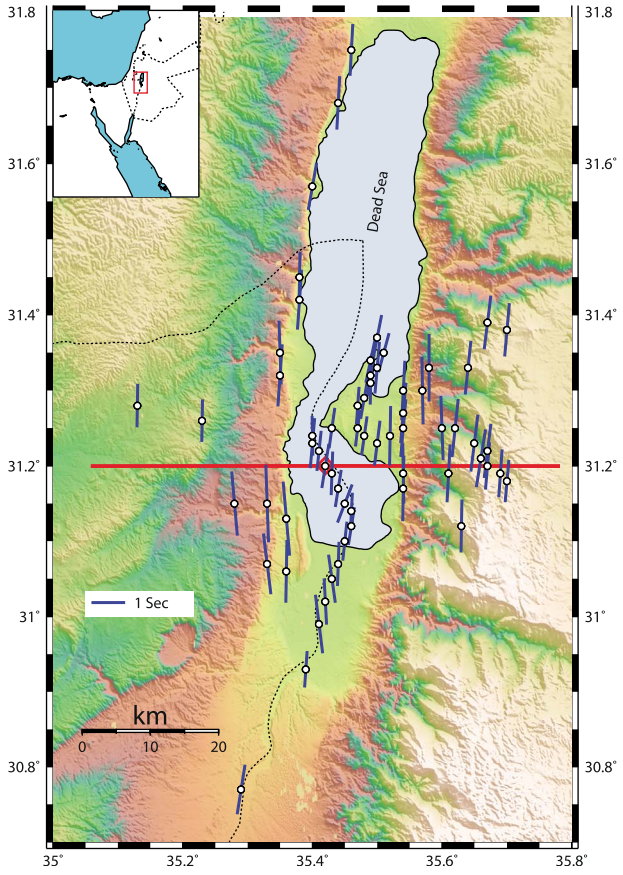

Figure 1. Average splitting parameters measured at the stations of the DESIRE network. The orientation of the blue bars indicates the fast axis with lengths scaled according to the delay times. The red solid line denotes the position of the profile on which the splitting parameters are projected.

part of the auxiliary material (Figure S1).[1] For this back-azimuthal range we obtained the largest number of non-null splitting measurements and we use the corresponding results as a basis for our modeling. The splitting parameters projected on an EW-trending profile illustrate that delay times decrease significantly in the center of the profile. The dominant wavelength of these variations is about 20 km. The corresponding fast-polarization directions are more-or-less constant. We also tested for the possible dependence of the splitting parameters on the dominant period and the initial polarization of the incoming shear wave. However, no significant variations of the delay times and fast axes are observed.

3. Full Waveform Modeling

[5] In order to explain the observed short-scale variations of splitting parameters, we use a 2-D finite difference approach to solve the complete wave equation for an elastic medium of orthorhombic symmetry. The a-axis of the orthorhombic medium is assumed to vary within the horizontal plane only, similar to the approach described by *Ryberg et al.* [2005]. The coordinate axes are chosen such that the model parameters (including the P- and S-wave isotropic reference velocities, percentage and horizontal symmetry axes of anisotropy, and density) change in the Z (depth) and E-W directions. A 63° initial polarization angle and a sinusoidal wavelet (1 period of 10 sec duration) is used to simulate the SKS wave propagating in our models. For a vertically-travelling incoming shear wave synthetic SKS seismograms are obtained at a linear array of receivers at the surface, simulating the E-W observation profile. We subsequently analyzed the synthetic seismograms in the same way as the real SKS waveforms to deduce the splitting parameters. Geophysical data [*Mechie et al.*, 2009; *Mohsen et al.*, 2010] suggest a ~35 km thick crust beneath the DSB with no significant uplift of the Moho. We use this value in our models and assume total thickness of the lithosphere and asthenosphere of 200 km. The computational domain is chosen large enough to avoid interferences with artificial reflections from the boundaries of the model. In our models and if not stated otherwise, the effective S-wave velocities in the crust and upper mantle are 3.5 km/s and 4.6 km/s respectively. The mantle part of the lithosphere (between 35 and 200 km depth) is assumed to exhibit an anisotropy of 4% (based on the relative difference between the fast and slow shear-wave velocity in the vertical direction). However, our modeling and the SKS-splitting measurements are not sensitive to the exact depth range of mantle anisotropy. The models are shown in Figures 2 and 3. In agreement with previous studies on anisotropy in the Dead-Sea region, we assume an N-S oriented symmetry axis in the mantle [*Rümpker et al.*, 2003; *Levin et al.*, 2006]. The studies also suggest that the anisotropic symmetry axis in the mantle beneath the region changes only moderately.

3.1. Lateral Variation of Elasticity in the Mantle

[6] In a first attempt to explain the observed lateral variation of splitting parameters we investigate the possibility of lateral changes in mantle elasticity.

3.1.1. Strength of Anisotropy

[7] The fast polarizations are relatively uniform along the profile, whereas the delay times are highly variable and exhibit relatively small values in the center. This may be taken as an indication for significantly reduced anisotropy. To study the corresponding waveform effects, we choose an extreme model with a 10-km wide isotropic region in the mantle beneath the center of the profile (Figure 2). In this model the crust is uniformly isotropic. Away from the center, anisotropy in the mantle is of uniform strength (4%). It is evident that variations of the synthetic splitting parameters are too subtle and do not fit the short-wavelength variations observed in the real data.

3.1.2. Effective Isotropic Velocity

[8] As an alternative possibility, we tested for the effect of the lateral variations in the (effective) isotropic velocity structure of the mantle. The model in Figure 3a consists of an anisotropic mantle with a narrow 4-km wide central zone of reduced effective S-velocity (4.2 km/s, corresponding to 8.5% reduction). Anisotropic parameters in this zone remain unchanged. Synthetic splitting parameters at distances of up to 50 km away from the center are still affected by the narrow zone of reduced velocities. While such a lateral heterogeneity in the isotropic structure of the mantle can have strong

[1] Auxiliary materials are available in the HTML. doi:10.1029/2010GL046464.

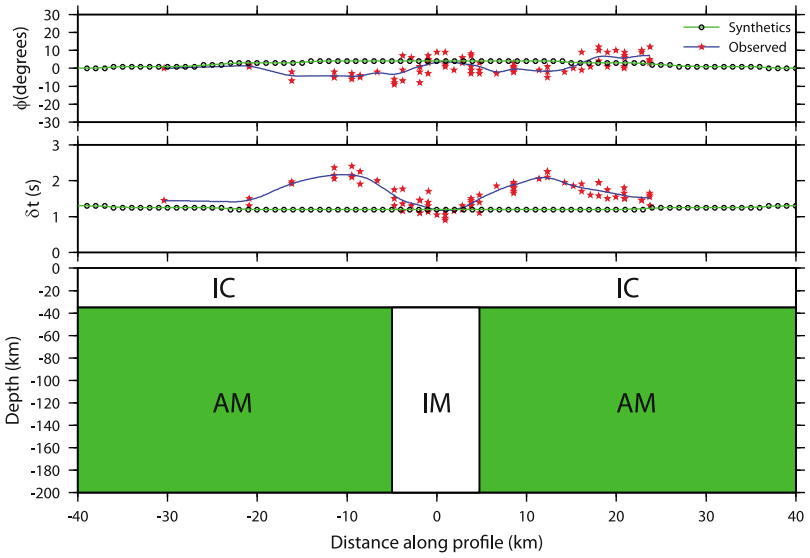

Figure 2. A model with lateral variation in the strength of mantle anisotropy only. Curves in the upper panel show variations of observed and synthetic splitting parameters. IC: homogeneous and isotropic crust, v_s = 3.5 km/s; AM: homogeneous and anisotropic mantle, effective v_s = 4.6, km/s, strength of anisotropy: 4%, orientation of the subhorizontal a-axis: 0°; IM: homogeneous and isotropic mantle, v_s = 4.6 km/s.

influences on the splitting parameters, it is not able to explain the small-scale variations observed across the DSB.

3.2. Lateral Variation of Elasticity in the Crust

[9] The previous examples show that lateral changes in mantle seismic properties alone are unlikely to have a significant impact on the observations. Therefore, in the following, we keep the mantle anisotropy uniform and consider models with variations in crustal elasticity only.

3.2.1. Strength and Symmetry of Anisotropy

[10] As an example of crustal variations we investigate effects for a model with a narrow 6-km wide central anisotropic zone within an otherwise isotropic crust (Figure 3b). The anisotropic parameters for this zone are chosen rather arbitrarily with a strength of 10% and a fast-axis orientation of N30°W. The splitting parameters for this model differ significantly from the observations. After having tested many models with different thickness and width of the anisotropic block and a variety of strengths and fast-axis orientations (further examples are given in the auxiliary material), we noticed that with solely lateral variations in the anisotropic structure in the crust and/or mantle we are unable to explain the observed short-distance strong variations in the delay times.

[11] In addition we examined cases (not shown here) where the anisotropy is restricted to the crust (without any contribution from the mantle). However the output of such models is generally similar to that shown in Figure 2. These extreme examples demonstrate that the observed characterization of the splitting parameters can not be explained by changes in the degree and symmetry of anisotropy in the crust beneath the DSB.

3.2.2. Effective Isotropic Velocity

[12] The DSB is characterized by deep reaching sediments and fractures. We therefore consider a model with lateral variations of isotropic velocity in the crust. A 6-km wide low-velocity block with S-wave velocity of 2.9 km/s (a reduction of 17%) is introduced beneath the DSB (Figure 3c). The model is based on the assumption that the shear zone beneath the pull-apart basin extends through entire crust. The low-velocity zone produces strong variations in the calculated splitting parameters. However, the dominant wavelength of the synthetic delay-time variations is about 40 km and thus too wide to fit the observations. We also tested other models with differences in the width and in the amplitude of the low-velocity anomaly. A wider section with less reduced velocity may generate minimum points of the delay times similar to those observed, however, the pattern remains of relatively long wavelength. On the other hand, for a more narrow section, the required velocity reduction becomes unrealistic.

3.2.3. Near-Surface Isotropic Velocity

[13] From the scenarios described above, we can conclude that the source of the observed splitting pattern across the DSB must be shallow and located within the upper crust, whereas variations of anisotropic properties seem to play a minor role. Therefore, we next assume strong lateral velocity heterogeneities in the upper crust. The model shown in Figure 3d exhibits a 12-km wide and 15-km deep low-velocity isotropic block within an otherwise homogeneous and isotropic crust overlying a homogeneous and uniformly anisotropic mantle. This low-velocity block with an S-wave velocity of 2.7 km/s simulates the sedimentary fill of the DSB. The delay times obtained for this model exhibit similar variations as those observed in the data. The model yields a variance reduction of 93% in δ t-misfit in comparison to the initial model (with reduced anisotropy in the central zone of the mantle) shown in Figure 2.

4. Discussion and Conclusions

[14] The different scenarios examined here reveal that any lateral change in the anisotropic structure alone at any depth in the mantle or crust is not able to explain the observed pattern of the splitting parameters across the DSB. On the other hand, models with significantly reduced isotropic velocity at shallow depth beneath the DSB provide the best

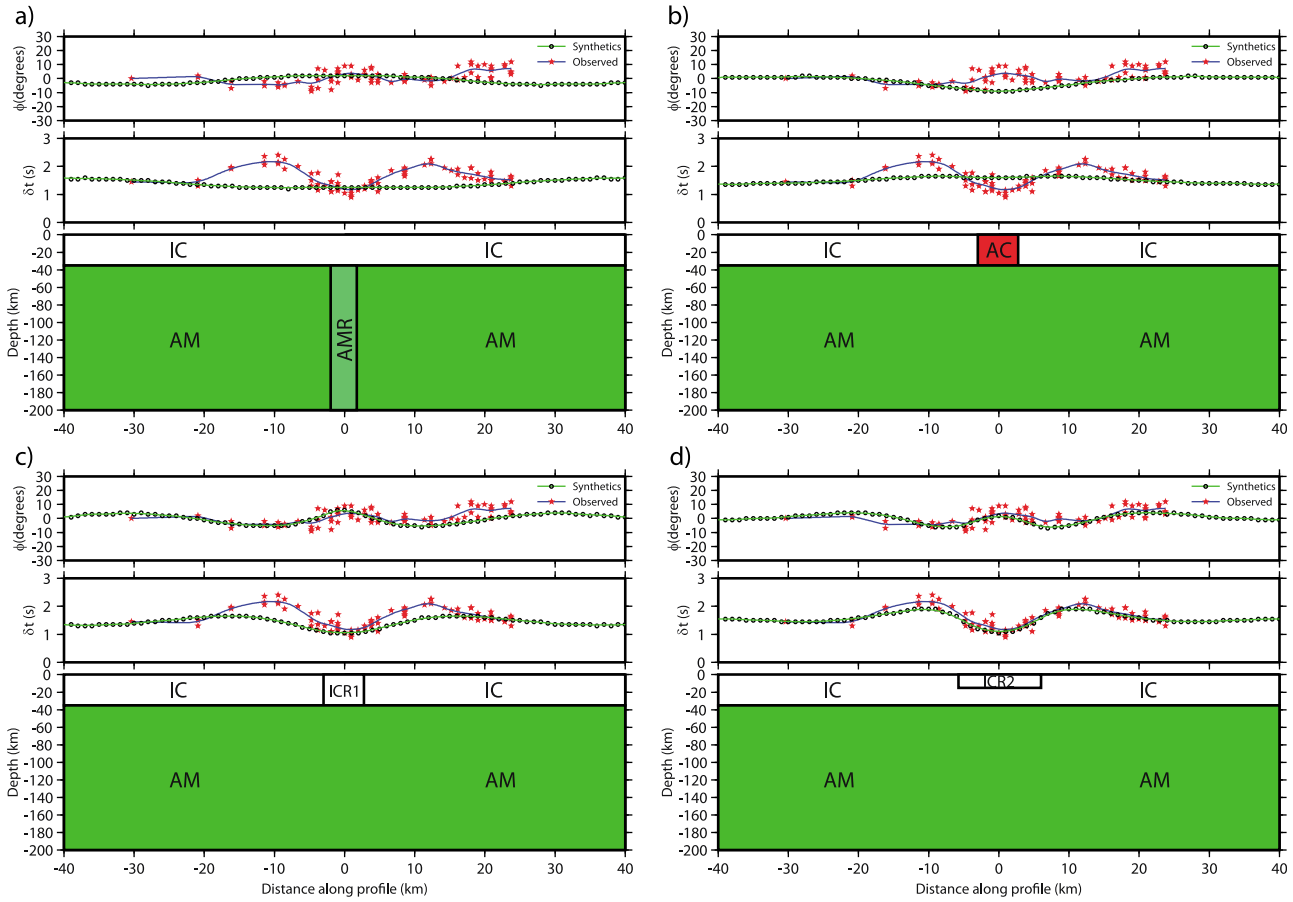

Figure 3. Models with lateral variations in the elasticity of the crust or mantle. The top two curves in each plot are as described in Figure 2. (a) Lateral variation in effective isotropic velocity in the mantle. The 4-km wide central section has lower velocity than the surrounding mantle. (b) Lateral variation in strength and a-axis of anisotropy in the crust. The 6-km wide central section is anisotropic within an otherwise isotropic crust. (c) Lateral variation in isotropic velocity in the crust. The 6-km wide central section has lower velocity than the surrounding crust. (d) Lateral variation in isotropic velocity at shallow depths. The 12-km wide and 15-km thick central section exhibits low velocity representing the sedimentary basin. IC: homogeneous and isotropic crust, $v_s = 3.5$ km/s; ICR1: isotropic crust of reduced velocity, $v_s = 2.9$ km/s; ICR2: isotropic crust of reduced velocity, $v_s = 2.7$ km/s; AC: anisotropic crust, effective $v_s = 3.5$ km/s, strength of anisotropy: 10%, horizontal a-axis: N30°W; AM: homogeneous and anisotropic mantle, $v_s = 4.6$, km/s, strength of anisotropy: 4%, horizontal a-axis: N0°E; AMR: Anisotropic mantle with reduced effective velocity, $v_s = 4.2$ km/s, strength of anisotropy: 4%, horizontal a-axis: N0°E.

fit to the observations. The shallow low-velocity section in the model simulates the thick sedimentary fill in the basin. These findings are in agreement with results obtained by *Mohsen et al.* [2010] from receiver function analysis of the DESIRE network and also with the earlier results from seismic refraction [*Ginzburg and Ben-Avraham*, 1997] and thermo-mechanical modeling [*Petrunin and Sobolev*, 2006].

[15] We also examined effects of changes in the lateral and vertical extent of the central section. However, models, where the central section extends over the whole thickness of the crust produce relatively long-wavelength variations of splitting parameters (Figure S3 in the auxiliary material). Further tests reveal that possible, more-complex, geometries of the shallow low-velocity section, as inspired by results of *Ben-Avraham et al.* [2008] (see Figure S4 in the auxiliary material), cannot be resolved, due to the relatively large dominant period of the SKS phases. We did not account for 3-D complexities in our models, however, the agreement between observed splitting parameters and results obtained for the final model (Figure 3d) suggests that the anisotropic structure beneath the DSB is mainly controlled by 2-D structural variations.

[16] While the observations exhibit significant variations in delay time along the profile, fast polarization are relatively uniform. Synthetic tests show that anisotropic models with changes in symmetry-axes orientation also cause significant variations in delay times [e.g., *Hammond et al.*, 2010]. We tested models with lateral changes in the symmetry axes of anisotropy. However, to generate the observed variations of the delay times, we required a change in the symmetry axis orientation in the order of 90°. Such significant variations are not supported by our fast-polarization observations.

[17] Our modeling shows that strong lateral variations in the isotropic velocity near the surface are responsible for the small-scale variations in the observed splitting. This is related to the fact that the laterally varying structure affects orthogonally polarized shear waves differently. As a result,

when the scale of the heterogeneities is smaller than the dominant wavelength of the shear-wave, the heterogeneities can cause effective anisotropy [*Marson−Pidgeon and Savage*, 1997]. On the other hand, larger-scale heterogeneities may cause scattering and reduce the effective splitting [*Wu*, 1989]. In our models the low velocity zone covers a range of 12 km in the E-W direction, whereas it extends infinitely in the N-S direction. The dominant wavelength of the SKS phase of approximately 30 km is larger than the scale length of the heterogeneities. In this case effective-medium properties become important and infinite-frequency approximations break down. The related wavefield modifications can only be described by more-complete approaches similar to the finite difference modeling presented here.

[18] *Rümpker et al.* [2003] and *Ryberg et al.* [2005] present variations of the splitting parameters along a 200-km linear array of stations across the DST about 75 km south of DSB. Their modeling suggests lateral changes in the anisotropic structure of the crust and upper mantle in relation to a boundary-layer shear zone accommodating the relative motion along the DST. Our results suggest that the significant crustal anisotropy in their models, to a certain degree, may be reduced by considering effects of isotropic lateral variations. However, geophysical data [see *Weber et al.*, 2009, and references therein] indicate that the sedimentary cover is only 4 km thick and less wide in that part of the DST.

[19] The dense network of stations allowed us to identify the shallow-depth source of the observed small-scale variations in splitting parameters. The short length of the profile of only 60 km, however, prevents us from drawing any further conclusions on possible anisotropic variations in the mantle beneath the DSB. The main questions regarding the depth and lateral extend of the anisotropic structures in direct relation and neighborhood to the DSB, therefore, remain to be answered. The modeling suggests that the contribution of crustal anisotropy is not significant to the observations presented here. In a forthcoming paper we will extend our investigation by combining the available shear-wave splitting data from the regional DESERT and DESIRE seismic networks to further resolve the anisotropic elastic properties beneath them.

[20] **Acknowledgments.** We thank the Geophysical Instrument Pool Potsdam (GIPP) for providing the seismic stations used in the experiment. AK was funded by the German Research Foundation (DFG). We are grateful to two anonymous reviewers for detailed comments and suggestions.

References

Ben-Avraham, Z., Z. Garfunkel, and M. Lazar (2008), Geology and evolution of the southern Dead Sea fault with emphasis on subsurface structure, *Annu. Rev. Earth Planet. Sci.*, *36*, 357–387, doi:10.1146/annurev.earth.36.031207.124201.

Bowman, J. R., and M. Ando (1987), Shear-wave splitting in the upper-mantle wedge above the Tonga subduction zone, *Geophys. J. R. Astron. Soc.*, *88*, 25–41, doi:10.1111/j.1365-246X.1987.tb01367.x.

Garfunkel, Z. (1981), Internal structure of the Dead Sea leaky transform (rift) in relation to plate kinematics, *Tectonophysics*, *80*, 81–108, doi:10.1016/0040-1951(81)90143-8.

Ginzburg, A., and Z. Ben-Avraham (1997), A seismic refraction study of the north basin of the Dead Sea, Israel, *Geophys. Res. Lett.*, *24*(16), 2063–2066, doi:10.1029/97GL01884.

Hammond, J. O. S., J. M. Kendall, D. Angus, and J. Wookey (2010), Interpreting spatial variations in anisotropy: Insights into the Main Ethiopian Rift from SKS waveform modelling, *Geophys. J. Int.*, *181*, 1701–1712, doi:10.1111/j.1365-246X.2010.04587.x.

Levin, V., A. Henza, J. Park, and A. Rodgers (2006), Texture of mantle lithosphere along the Dead Sea Rift: Recently imposed or inherited?, *Phys. Earth Planet. Inter.*, *158*, 174–189, doi: 10.1016/j.pepi.2006.05.007.

Marson-Pidgeon, K., and M. K. Savage (1997), Frequency-dependent anisotropy in Wellington, New Zealand, *Geophys. Res. Lett.*, *24*(24), 3297–3300, doi:10.1029/97GL03274.

Mechie J., K. Abu-Ayyash, Z. Ben-Avraham, R. El-Kelani, I. Qabbani, M. Weber, and DESIRE Group (2009), Crustal structure of the southern Dead Sea basin derived from project DESIRE wide-angle seismic data, *Geophys. J Int.*, *178*, 457–478, doi:10.1111/j.1365-246X.2009.04161.x.

Mohsen, A., G. Asch, J. Mechie, R. Kind, R. Hofstetter, M. Weber, M. Stiller, and K. Abu-Ayyash (2010), Crustal structure of the Dead Sea Basin (DSB) from a receiver function analysis, *Geophys. J Int.*, *184*, 463–476, doi:10.1111/j.1365-246X.2010.04853.x.

Petrunin, A., and S. V. Sobolev (2006), What controls thickness of sediments and lithospheric deformation at a pull-apart basin?, *Geology*, *34*, 389–392, doi:10.1130/G22158.1.

Rümpker, G., T. Ryberg, G. Bock, and Desert Seismology Group (2003), Boundary-layer mantle flow under the Dead Sea transform fault inferred from seismic anisotropy, *Nature*, *425*, 497–501, doi:10.1038/nature01982.

Ryberg, T., G. Rümpker, C. Haberland, D. Stromeyer, and M. Weber (2005), Simultaneous inversion of shear wave splitting observations from seismic arrays, *J. Geophys. Res.*, *110*, B03301, doi:10.1029/2004JB003303.

Silver, P. G., and W. W. Chan (1991), Shear wave splitting and subcontinental mantle deformation, *J. Geophys. Res.*, *96*(B10), 16,429–16,454, doi:10.1029/91JB00899.

Sobolev, S. V., A. Petrunin, Z. Garfunkel, A. Y. Babeyko, and the DESERT Group (2005), Thermo-mechanical model of the Dead Sea Transform, *Earth Planet. Sci. Lett.*, *238*, 78–95, doi:10.1016/j.epsl.2005.06.058.

ten Brink, U. S., A. S. Al-Zoubi, C. H. Flores, Y. Rotstein, I. Qabbani, S. H. Harder, and G. R. Keller (2006), Seismic imaging of deep low-velocity zone beneath the Dead Sea basin and transform fault: Implications for strain localization and crustal rigidity, *Geophys. Res. Lett.*, *33*, L24314, doi:10.1029/2006GL027890.

Weber, M., et al. (2009), Anatomy of the Dead Sea Transform from lithospheric to microscopic scale, *Rev. Geophys.*, *47*, RG2002, doi:10.1029/2008RG000264.

Wu, R. S. (1989), Seismic wave scattering, in *The Encyclopedia of Solid Earth Geophysics*, edited by D. James, pp. 1166–1187, Van Nostrand-Reinhold, New York.

G. Asch and M. Weber, Deutsches GeoForschungsZentrum Potsdam, Telegrafenberg, D-14473 Potsdam, Germany. (asch@gfz-potsdam.de; mhw@gfz-potsdam.de)

A. Kaviani and G. Rümpker, Institute of Geosciences, Goethe-University Frankfurt, Altenhöferallee 1, D-60438 Frankfurt, Germany. (kaviani@geophysik.uni-frankfurt.de; rumpker@geophysik.uni-frankfurt.de)